Available online at www.sciencedirect.com
SCIENCE DIRECT®
Journal of Pharmaceutical and Biomedical Analysis
35 (2004) 93–105
JOURNAL OF PHARMACEUTICAL AND BIOMEDICAL ANALYSIS
www.elsevier.com/locate/jpba

Integrated application of transcriptomics and metabonomics yields new insight into the toxicity due to paracetamol in the mouse

Muireann Coen [a], Stefan U. Ruepp [b,1], John C. Lindon [a,*], Jeremy K. Nicholson [a], François Pognan [c], Eva M. Lenz [d], Ian D. Wilson [d]

[a] *Biological Chemistry, Biomedical Sciences Division, Faculty of Medicine, Imperial College, Sir Alexander Fleming Building, South Kensington, London SW7 2AZ, UK*
[b] *Department of Safety Assessment, AstraZeneca Pharmaceuticals, Mereside, Alderley Park, Macclesfield, Cheshire SK10 4TG, UK*
[c] *Department of Safety Assessment, AstraZeneca Pharmaceuticals, Wilmington, DE 19850, USA*
[d] *Department of Drug Metabolism and Pharmacokinetics, AstraZeneca Pharmaceuticals, Mereside, Alderley Park, Macclesfield, Cheshire SK10 4TG, UK*

Received 25 November 2003; received in revised form 15 December 2003; accepted 15 December 2003

Abstract

Gene chip array (Affymetrix) data from liver tissue and high resolution ^{1}H NMR spectra from intact liver tissue, tissue extracts and plasma have been analyzed to identify biochemical changes arising from hepatotoxicity in mice dosed with acetaminophen. These data sets have been co-interpreted in terms of common metabolic pathways. The principal metabolic changes comprised a decrease in hepatic glucose and glycogen in intact tissue, coupled with an increase in lipid content, with increases in the levels of glucose, pyruvate, acetate and lactate in plasma, and increases in alanine and lactate in the aqueous tissue extracts. Collectively these data provide evidence for an increased rate of hepatic glycolysis. The metabolic observations were consistent with the altered levels of gene expression relating to lipid and energy metabolism in liver which both preceded and were concurrent with the metabolic perturbations. The results show that these two technology platforms together offer a complementary view into cellular responses to toxic processes, providing new insight into the toxic consequences, even for well-studied therapeutic agents such as acetaminophen.

Keywords: Transcriptomics; Metabonomics; NMR; Toxicity; Paracetamol; Liver; Plasma

Abbreviations: ALT, alanine aminotransferase; ANOVA, analysis of variance; APAP, acetaminophen; AST, aspartate aminotransferase; CPMG, Carr-Purcell-Meiboom-Gill; EDTA, ethylenediaminetetraacetic acid; HMQC, heteronuclear multiple quantum coherence; MAS, magic angle spinning; NCBI, National Center for Biotechnology Information; NMR, nuclear magnetic resonance; PCA, principal components analysis; PCR, polymerase chain reaction; RTQ, real time quantitative; TOCSY, total correlation spectroscopy; TSP, 3-(trimethylsilyl)-[2,2,3,3-$^{2}H_4$]-propionic acid sodium salt; VLDL, very low density lipoprotein

* Corresponding author. Tel.: +44-20-7594-3194; fax: +44-20-7594-3066.
E-mail address: j.lindon@imperial.ac.uk (J.C. Lindon).
[1] Present address: Non-Clinical Drug Safety, F. Hoffmann-La Roche Ltd., 4051 Basel, Switzerland.

0731-7085/$ – see front matter © 2004 Elsevier B.V. All rights reserved.
doi:10.1016/j.jpba.2003.12.019

1. Introduction

There is now increasing pressure on pharmaceutical companies to develop approaches that will enable personalized healthcare through the use of pharmacogenomics. This approach will be used as a basis to select patients in order to minimize side effects and to maximize therapeutic efficacy. In addition, in order to reduce drug candidate attrition at the preclinical stage, new technologies such as toxicogenomics are being used in an attempt to select optimum candidates for further development. This is despite some uncertainty over the meaning of changed gene expression profiles in relation to drug toxicity end-points and, therefore, validation strategies are needed. One approach is to study the metabolic consequences of a pathological process and relate these to the gene expression profiles even though the two processes may occur on different time scales. We show here that metabonomics data and gene expression changes, both as a function of dose and time after treatment, that result from administration of paracetamol (acetaminophen), a widely used drug, relate in many cases to the same biochemical pathways. The effects can be related to each other in a consistent fashion and although they occur, as has been predicted [1], at different times after the xenobiotic administration, the subsequent metabonomic changes provide validation of the earlier gene expression alterations.

New technology platforms, generating high volumes of data, are being increasingly applied in the search for novel biomarkers and deeper understanding of toxic effects of drugs. In addition to genomics and proteomics platforms, metabonomics, which has been defined as 'the study of multiparametric metabolic responses in living systems after pathophysiological stimuli or genetic modification' [1–3], is becoming more widely used in xenobiotic safety assessment in the pharmaceutical industry [4,5]. This approach of combining data comprising simultaneous detection of multiple analytes with computer-based pattern recognition and classification methods has been applied to the investigation of perturbed metabolic profiles in biofluids using conventional solution state NMR spectroscopy [2,3] and intact biological tissues using magic-angle-spinning (MAS) NMR spectroscopy [6–8]. These approaches can provide detailed information about their biochemical composition, allowing identification of target organ of toxicity, time courses of development of, and regeneration from a toxic lesion and identification of biomarker combinations. It has been shown recently that integrated metabonomic analysis of both tissues and biofluids is useful in mechanistic toxicological studies [7,9].

Paracetamol (acetaminophen, *N*-acetyl-*p*-aminophenol) is a widely used anti-pyretic, analgesic drug, which after high doses can result in centrilobular hepatic necrosis with occasional observation of nephrotoxicity [10–13], and the mechanism of toxicity has been characterized [14,15]. Additionally, ^{1}H NMR spectroscopy of urine has been used to investigate the biochemical sequelae of the toxic process in the overdose situation [16]. In the present study, metabonomic and gene expression analyses have been applied together for mutual validation of the dose- and time-dependent responses in liver tissue from mice dosed with various levels of paracetamol. The techniques used comprised Affymetrix gene transcript profiling and MAS ^{1}H NMR spectra of intact liver, together with high resolution ^{1}H NMR spectra of tissue extracts and plasma samples.

The combination of metabonomic and transcriptomic analysis leads to improved understanding of the time-related biochemical consequences of the drug toxicity and constitutes a new approach for the investigation of drug safety.

2. Materials and methods

2.1. Samples

All animal procedures were performed in accordance with current UK legislation. Alderley Park (AP-1) male mice were fasted overnight and remained fasted after an i.p. injection of paracetamol in sterile 0.9% (w/v) saline solution. Ten mice were injected with vehicle (control, 0 mg/kg paracetamol), 20 mice each received 50, 150 or 500 mg/kg of paracetamol. The animals were euthanized by CO_2 inhalation at varying time points of 15, 30, 60, 120, and 240 min after dosing. The doses of 50, 150, and 500 mg/kg were selected because they were expected to give a gradation of the transcriptional and metabolic responses following pharmacological, sub-toxic and toxic exposures. The livers were removed immediately, weighed

and cut into four parts. A sub-sample of each of the four major lobes (left and right lateral, left and right medial lobes) was taken and fixed in buffered formalin. One histological section was prepared from each sample, stained with H and E and examined by light microscopy. Other sub-samples were snap-frozen in liquid nitrogen and stored at −80 °C until required for analysis. Blood samples were withdrawn by cardiac puncture and placed in EDTA-coated tubes from which plasma samples were isolated by centrifugation. ALT and AST activities, and the paracetamol plasma concentration, were quantified using colorimetric methods (Sigma 505, 505-P and 430-A kits, respectively).

2.2. Gene expression analysis

The murine 11K set was used for transcript profiling (Affymetrix, Santa Clara, CA). Total RNA from individual mouse livers was purified by a standard method [17], and identical amounts of RNAs from mice within each group were pooled, labeled, and processed according to the manufacturer's instructions. RNA purification and every step of cRNA generation was quality checked by agarose gel electrophoresis. The quality of the fragmented cRNA was further assessed using TestII Chips from Affymetrix. Primary data were collated using Microarray Suite Version 4.0.1 software (Affymetrix, Santa Clara, CA). The software calculates the fluorescence intensity values (after background subtraction) for each of the perfect-match (PM) and mismatch (MM) 25-mer oligonucleotide probe pairs designed for each gene or EST cluster [18]. The average difference between the PM and MM values of each gene provide a relative, but quantitative assessment of the mRNA abundance [19]. The software also scores whether a transcript is present (P) or absent (A) on the chip. In order to allow comparison between chips, expression values were scaled to a defined target intensity of 250. Scaling multiplies the average intensity on an array with a factor (scaling factor) to the target intensity. The chips from group 9 (control group 60 min) were chosen as baseline files for calculation of fold-changes by the Microarray Suite software. Fold-change was calculated as the ratio of each group divided by the median of the five control groups. Genes were identified as up-regulated if at least two out of the five time groups at 500 mg/kg paracetamol were at least two-fold up-regulated and at least two out of five time groups at 500 mg/kg paracetamol were termed present. In order not to miss genes that changed only at the latest time point, genes that also showed at least five-fold up-regulation at 240 min and were termed present, were included. In both cases only genes that had in total less than 15 absent calls were included. Genes were identified as down-regulated if at least two out of the five time groups at 500 mg/kg paracetamol were at least two-fold down-regulated and at least two out of the five time groups at 500 mg/kg paracetamol were termed present. Again, genes that showed considerable down-regulation (more than five-fold) at the latest time point at the highest dose were also included. Genes that fulfilled one of the previous criteria and had less than four present calls in the five control groups were excluded. Additional annotation and information concerning pathway and molecular function was retrieved using public and proprietary databases.

2.3. RTQ-PCR

Total RNA (20 μg) from individual animals (only animals at euthanasia times of 15, 120, and 240 min) was treated with DNase I (Roche Diagnostics, Lewes, UK) for 30 min at 37 °C. RNA concentrations and purity were determined by using a spectrophotometer. Total RNA (4 μg) from individual animals was subsequently reverse transcribed at 42 °C for 50 min using Superscript II and oligo $dT_{12–18}$ (Life Technologies, Paisley, UK). Equal amounts of RNA from the six control animals were pooled and used to generate cDNA for the standard curve according to the same protocol. Absence of DNA contamination was confirmed by performing reverse transcription reactions, but without reverse transcriptase followed by RTQ-PCR analysis. Resulting first-strand cDNA was diluted 20-fold and 200-fold. An aliquot (1 μl) was used as a template for RTQ-PCR analysis which was carried out using a Light Cycler (Roche Diagnostics, Lewes, UK). Sequence-specificity of selected primers was confirmed by sequence similarity comparison with public and proprietary databases using BLAST 2 (NCBI). A relative standard curve of control group cDNA was used in each PCR reaction at the following dilutions: 1:2, 1:4, 1:8, 1:16, 1:32, 1:64, 1:128 and 1:256. Based on the expected fold up-regulation

(indicated by chip analysis) the 1:20 or 1:200 dilutions were used for the PCR reactions. In every set of PCR reactions, a negative control reaction was included, substituting cDNA with H_2O. PCR reactions were analyzed by melting peak and melting curve analysis using the supplied Light Cycler Software Version 3 (Roche Diagnostics, Lewes, UK). Based on chip results GAPDH was used for normalization of input cDNA amounts. The following primer pairs (HPSF-grade from MWG-Biotech, Milton Keynes, UK) were used for PCR analysis:

Gene	Accession	Upper primer	Lower primer
c-fos	V00727	AGCGCAGAGCATCGGCA	TGAGAAGGGGCAGGGTG
GAPDH	M32599	CCCCACTAACATCAAATG	ATCCACAGTCTTCTGGGT

2.4. ^1H NMR spectroscopy

Each liver portion, weighing approximately 20 mg, was placed in a spherical cavity in a 4 mm MAS ZrO_2 rotor with insert and spun at 5 kHz at the magic angle and ^1H NMR spectra were measured at 600 MHz at 300 K. A small amount of 3-(trimethylsilyl)-[2,2,3,3-$^2H_4$]-propionic acid sodium salt (TSP) was added as a chemical shift reference ($\delta = 0$) and D_2O was added to provide a field-frequency lock. The CPMG spin-echo pulse sequence was used to measure ^1H MAS NMR spectra. Typical parameters are given in the figure caption. For plasma, 500 μl aliquots were diluted in a ratio of 1:1.5 with D_2O, 50 μl of a TSP/D_2O solution was added and samples were placed in 5 mm NMR tubes. ^1H CPMG NMR spectra of these samples were measured at 500 MHz. For extraction, pre-weighed liver tissue (100 mg) was homogenized in 50% acetonitrile and then centrifuged at 10,000 rpm for 6 min. The supernatant was collected, lyophilized and reconstituted in D_2O. A TSP/D_2O solution was added as before. The pellet that remained from the aqueous extraction procedure underwent lipid extraction using 75% $CHCl_3$/25% CH_3OH. The precipitated protein was spun down at 10,000 rpm for approximately 10 min. The solvent was removed by drying under a stream of nitrogen. The lipid-soluble extracts were reconstituted into deuterated chloroform/methanol ($CDCl_3$/CD_3OD) (3:1). Extracts were placed in 5 mm NMR tubes and ^1H NMR spectra of aqueous extracts were measured at 600 MHz using a standard pulse sequence for water peak suppression. Lipid extract ^1H NMR spectra were obtained at 600 MHz with no solvent suppression being necessary. In addition, to aid lipid peak assignments, both one-dimensional ^{31}P NMR spectra and two-dimensional inverse-detected ^1H–^{31}P NMR HMQC-TOCSY spectra were measured. The two-dimensional spectrum yields both the connectivity between the ^{31}P chemical shifts and the ^1H chemical shifts of protons coupled to the phosphorus directly, plus the ^1H–^1H connectivities along an unbroken chain of ^1H–^1H spin couplings. The detailed NMR experimental parameters are given in the figure caption.

2.5. Chemometrics

Each NMR spectrum over the range δ 0.4–6.0 was segmented into frequency regions 0.04 ppm wide and the spectral integral calculated for each region using AMIX version 2.0, (Bruker Biospin, Rheinstetten, Germany). Regions that contained the resonance from residual water (δ 4.7–5.06) were removed from the data tables. In all plasma spectra, EDTA gave rise to two ^1H NMR peaks in the intensity ratio 2:1 at δ 3.62 and 3.21 and regions covering the EDTA resonances were removed from the data table as was the region corresponding to a residual methanol resonance (δ 3.3–3.9) in lipid extracts. The intensity values corresponding to each NMR spectrum were normalized to the sum of all integrals in order to remove concentration differences between dilute and concentrated samples. PCA was used to investigate the NMR data, using the software package Simca-P 8.0 (Umetrics AB, Umeå, Sweden).

3. Results

3.1. Histopathology, liver enzyme, and plasma paracetamol levels

Plasma concentrations of paracetamol attained maximum observed values 15 min after dosing at

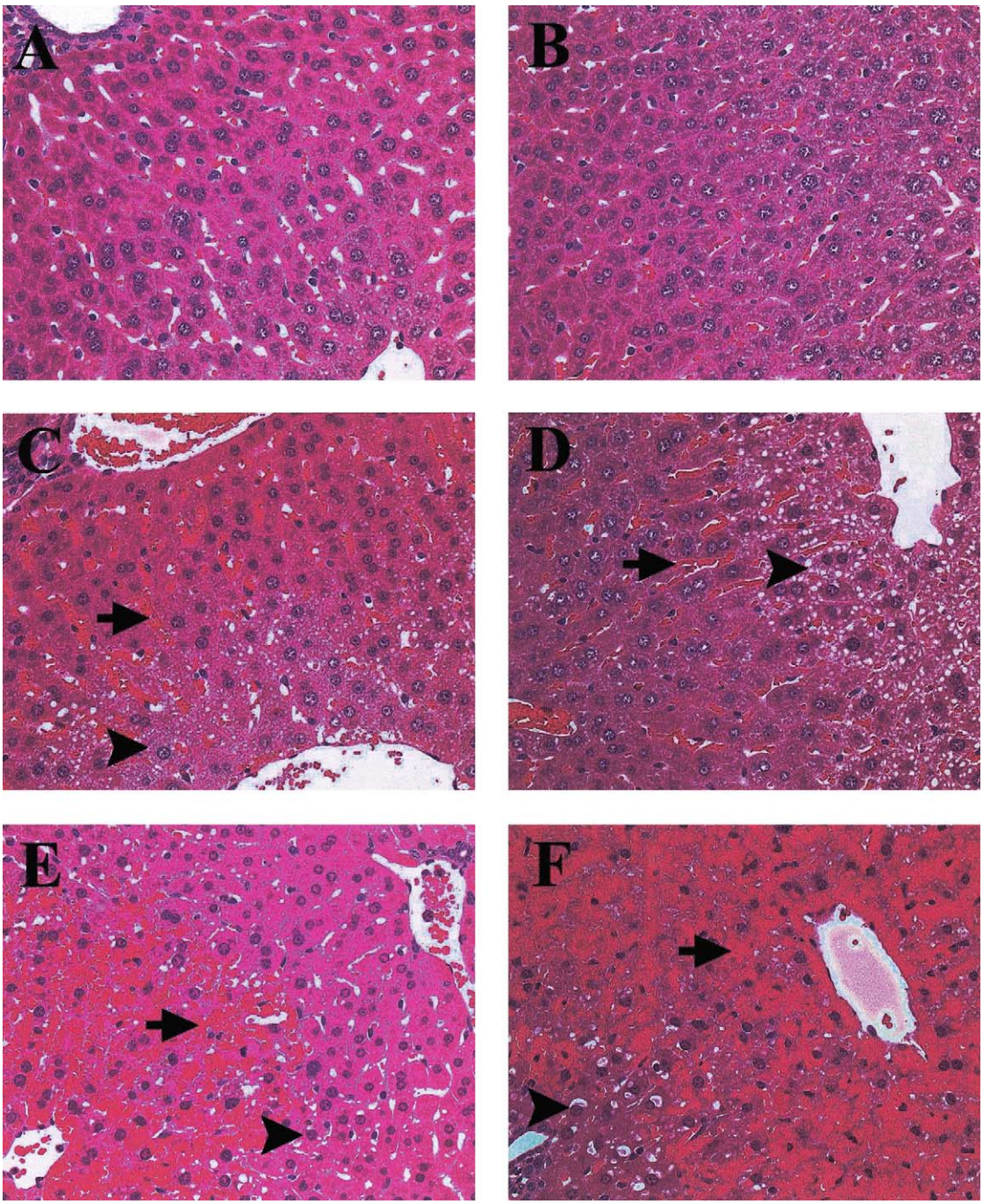

Fig. 1. Light microscopic photograph of H&E stained livers following paracetamol administration at 40-fold magnification: (A) control animal at 240 min post-injection; (B) animal treated with 50 mg/kg at 240 min post-injection; (C) animal treated with 150 mg/kg at 240 min post-injection; (D) animal treated with 500 mg/kg at 60 min post-injection; (E) animal treated with 500 mg/kg at 120 min post-injection; and (F) animal treated with 500 mg/kg at 240 min post-injection. Arrows indicate red cell congested sinusoids and arrowheads indicate vacuolated hepatocytes.

Table 1
Paracetamol plasma concentrations in mg/l

Time (min)	Dose (mg/kg)		
	50	150	500
15	26.5 ± 6.8*	77.0 ± 34 3*	350.6 ± 61.3**
30	44.6 ± 17.7*	78.8 ± 13.2**	317.9 ± 75 7**
60	14.3 ± 0.7	39.6 ± 8.4**	236.5 ± 60.5**
120	9.4 ± 3.5	16.9 ± 4.7	137.3 ± 18.2***
240	8.0 ± 2.1	9.0 ± 3.1	52.0 ± 21.7

The values given are average ± standard deviation. Plasma paracetamol background measurements obtained in control animals was 11.6 ± 4.6 mg/l. Statistical significance was calculated using a two-tailed, unequal variance *t*-test.

* $P < 0.05$.

** $P < 0.01$.

*** $P < 0.001$.

500 mg/kg and at 30 min at the two lower doses as indicated in Table 1. The toxic effects of paracetamol were evaluated using histopathology examination and the measurement of liver transaminases in plasma. Histopathological drug-related changes (swollen and vacuolated hepatocytes accompanied with sinusoids narrowing, leading to red blood cell congestion) observed by light microscopy as shown in Fig. 1 were visible at 240 min at 150 mg/kg and from 60 min onward at 500 mg/kg (Fig. 1(C)–(F)). No changes were observed at any time at 50 mg/kg (Fig. 1B). Determination of plasma ALT and AST levels indicated liver damage at the 500 mg/kg dose from 120 min onwards and at 240 min at the 150 mg/kg dose based on AST alone as summarized in Fig. 2. No statistical increase in these enzymes was observed at the 50 mg/kg dose. These findings were virtually identical to those obtained in a previous study [20], where, in addition, mitochondrial swelling was observed by electron microscopy as early as 15 min post-injection at a dose level of 500 mg/kg. All control liver samples were within normal limits at all time points.

3.2. Gene expression assays

Affymetrix mouse Mu11K chips were used to monitor gene expression changes and the affected genes were allocated to different pathway and different molecular function categories using public and proprietary databases. Some genes also showed considerable variation within the control and the 50 mg/kg

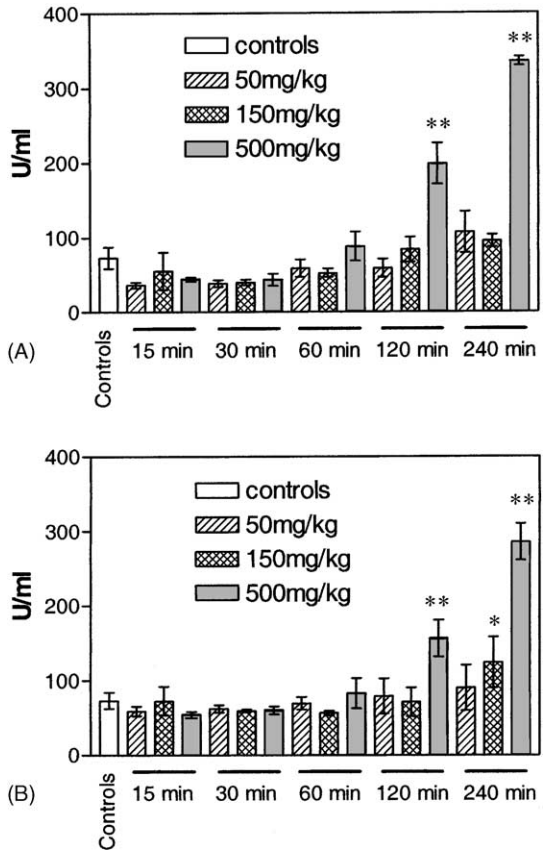

Fig. 2. Plasma hepatic transaminase levels as a function of time and dose of paracetamol: (A) ALT values; (B) AST values; $n = 10$ for controls and $n = 4$ for all other groups. Statistical significance was calculated by one-way ANOVA analysis.

paracetamol treated animal groups, and were therefore not further considered. The genomics results obtained were similar to those published earlier [20], although the Affymetrix chips used here contained many more identified genes than the custom-made nylon array previously used. As c-fos mRNA has been reported to be induced after toxic dosing of paracetamol [20,21], this gene was also monitored by quantitative RT-PCR and the kinetics of expression compared to the Affymetrix data where Fig. 3(A) shows the Affymetrix data and Fig. 3(B)) gives the RT-PCR results. The similarity in shape and fold induction provide confidence for the validity of the general fold inductions observed on microarray chips for other genes. However, it is not possible to assert that other

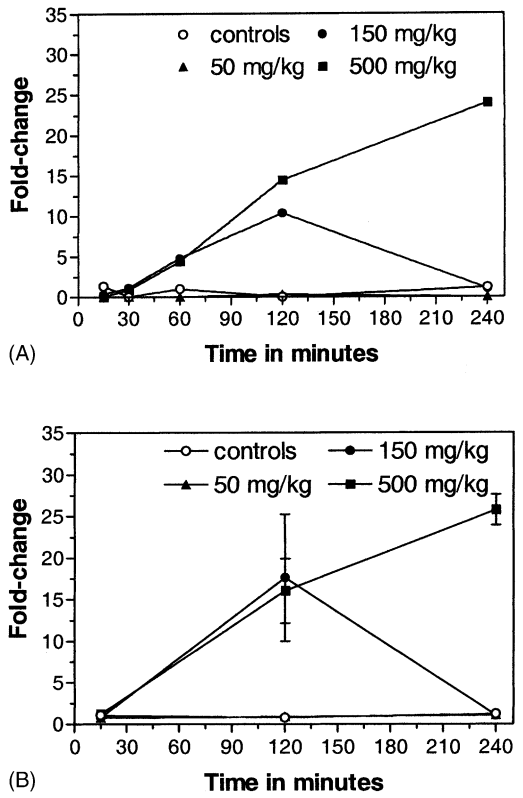

Fig. 3. Kinetics of c-fos expression as a function of time and dose of paracetamol: (A) Affymetrix data; (B) RTQ-PCR.

gene fold inductions would follow the same behavior.

The primary mechanism of paracetamol toxicity is believed to be chemically initiated through production of NAPQI by cytochrome P450 metabolism [14], leading to mitochondrial impairment and global energy failure [9,20]. Previously, it was shown that mitochondrial proteins involved in lipid metabolism and energy metabolism were mostly decreased. Similar results were obtained in the present study at the gene transcription level and so only lipid metabolism and energy metabolism genes are reported here as shown in Table 2. Lipoprotein lipase and VLDL protein receptor mRNAs were both down-regulated to a similar extent at all doses and all time points, being thus an early event in the pharmacology of paracetamol, as the low dose was shown to be non-toxic. It is likely that the VLDL mRNA decrease was an attempt to reduce the triglyceride import into the liver. Likewise, the decrease of fatty acid binding protein, which is a C18-fatty acid transporter, may be related to the same attempt to reduce fat accumulation in liver, due to inhibition of oxidative phosphorylation [20]. These changes are not thought to be responsible for the toxic injury, but at the high dose, combined with other gene regulations, they might increase paracetamol toxicity. Choline kinase was more likely to be linked to paracetamol toxicity, as its mRNA was up-regulated at mid- and high-doses from 120 min onward. This enzyme links choline to triglyceride metabolism and it is possible that this up-regulation was either an attempt to use the accumulating triglycerides in liver or was part of the building up of triglyceride.

It was hypothesized that production of glucose by β-*N*-acetyl-hexosaminidase was likely diminished because of the marked down-regulation of its mRNA production at the latest time point studied at the high dose. This enzyme is part of several pathways for the degradation of GM2 gangliosides. Although not the major source of glucose in metabolism, this would contribute to the overall energy failure and can be seen as a toxic event. ATP-synthase-γ-chain mRNA was decreased at the high dose, as were the α chain proteins in a proteomics investigation [20], and this would further contribute to an energy decrease in liver.

3.3. NMR-based metabonomics

The dose-dependence and the time-dependence of the metabonomic data have also been published recently [9] and are thus only summarized here. Typical ^{1}H MAS NMR spectra of intact liver tissue from control and high dose animals, euthanized 240 min after administration, are shown in Fig. 4(a) and 4(b)), respectively. The spectra from control tissues (Fig. 4(a)) are dominated by strong resonances from lipid triglycerides, glucose and glycogen, whilst the spectra from high dose animal tissues show mainly lipid peaks (Fig. 4(b)). The spectra also contained resonances corresponding to small molecules such as alanine, choline, phosphorylcholine, valine, glutamine, glutamate, trimethylamine-*N*-oxide (TMAO) and betaine. Differential biochemical effects are observed in Fig. 4(b) showing significant increases in the triglyceride resonances, a small decrease in the phospholipid content as measured using the $-N^{+}Me_3$ head-group of choline-containing phospholipids, and marked decreases in the glucose, glycogen, alanine,

Table 2
Gene expression fold changes as a result of paracetamol administration

	Dose (mg/kg)														
	50					150					500				
	Time (min)					Time (min)					Time (min)				
	15	30	60	120	240	15	30	60	120	240	15	30	60	120	240
Lipid metabolism															
Lipoprotein lipase	−1.0	−2.0	−1.3	−1.9	−2.6	−1.4	−1.4	−1.8	−2.0	−3.2	−2.8	−1.9	−1.6	−2.1	−3.2
VLDL receptor	−1.3	−3.5	−2.0	−1.3	−1.4	−1.0	−1.2	1.3	−1.3	−1.6	1.4	−1.2	−1.3	−3.3	−2.1
Fatty acid binding protein FABP/C-FAPB homologue	−24	−1.6	−4.5	−1.8	−1.6	−1.1	1.4	−1.0	−1.5	−2.4	−1.2	−1.1	−3.1	−1.6	−2.0
Fatty acid binding protein FABP/C-FAPB homologue	−2.1	−2.7	−2.1	−1.6	−1.0	−2.0	1.1	−1.0	−1.7	−1.2	1.1	−1.8	−2.1	−2.1	1.2
HMG-CoA reductase	−1.2	−1.8	−2.1	−0.6	−2.6	−1.5	−1.1	1.1	−1.2	1.1	−1.6	−1.9	−2.2	−2.2	−1.4
Choline kinase	2.1	1.3	1.6	1.1	1.4	2.0	1.3	1.7	3.0	3.9	1.7	1.3	1.0	2.1	5.7
Oxysterol-binding protein	1.4	1.1	2.6	3.3	1.3	1.8	2.3	2.5	2.9	2.2	1.8	1.5	4.3	2.3	4.0
Uteroglobin	0.9	1.3	1.8	3.0	1.1	1.1	1.6	1.9	1.7	1.5	2.1	1.7	2.1	1.8	2.2
Energy metabolism															
ATP synthase γ-subunit, mitochondrial	−1.5	−1.2	−1.1	−1.1	−1.0	−1.0	−1.0	−1.5	−1.3	−1.1	−1.1	−1.2	−1.1	−2.0	−2.1
β-*N*-acetylhexosaminidase α-subunit	−2.0	−1.4	1.3	1.3	−1.4	2.0	1.1	1.7	2.0	1.7	1.3	1.7	1.7	1.1	−23.5
Cholesterol α-7-hydroxylase	−1.4	−1.9	−2.3	−1.2	2.0	−1.2	−1.4	−1.8	−1.7	1.4	−1.7	1.1	−1.6	−2.4	−4.3
Cytochrome C oxidase subunit VII	−1.1	−1.4	−1.2	−1.2	1.1	1.1	1.1	−1.1	1.0	1.3	−2.2	−1.1	−1.4	1.1	−2.1
Glucosamine-6-phosphate isomerase	−1.3	−4.3	−1.2	1.7	2.5	−3.3	−1.0	1.4	1.0	1.3	3.3	1.4	−1.3	−1.8	−6.5
Insulin-like growth factor binding protein (IGFBP-1)	2.2	1.3	1.7	0.5	0.5	0.5	2.0	0.7	2.3	2.2	1.1	1.4	1.3	3.8	4.9
ATP synthase protein 8	−1.1	−1.0	−1.3	3.0	−1.3	27	1.5	2.4	1.9	1.5	1.3	2.7	4.2	1.9	2.7

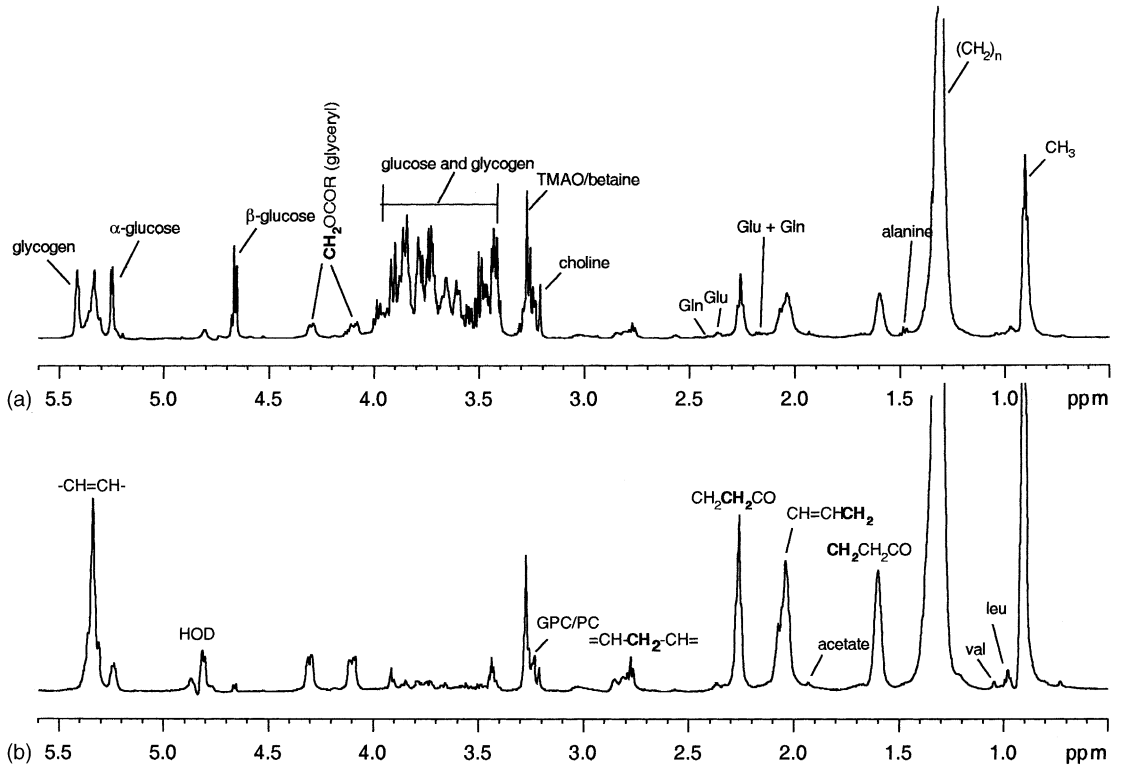

Fig. 4. (a) 600 MHz MAS ^{1}H CPMG NMR spectrum of control mouse liver tissue (spin-echo relaxation delay 40 ms, 128 scans, 32 K data points, spectral width 12 kHz, relaxation delay 5 s, acquisition time 2.13 s, line broadening factor 0.3 Hz); (b) 600 MHz MAS ^{1}H CPMG NMR spectra of mouse liver tissue from an animal dosed with paracetamol at 500 mg/kg and sampled at 240 min.

and choline resonances at this time point and dose level. The result at the 150 mg/kg dose was similar although the scale of the changes was less.

These metabolic alterations were also observed at the 60 and 120 min time points for the middle and high dose groups. At the lowest dose, at 240 min post-dose, the glycogen resonance was decreased but no other effects were observed. Peaks from paracetamol glucuronide also appeared in the ^{1}H MAS NMR spectra of intact liver from the high dose animals from 60 min onwards.

The combined use of NMR spectroscopy and multivariate statistical analysis methods has been shown to be useful for the analysis of metabolic changes in complex spectra particularly from biofluids [22–24]. Here a PC trajectory plot for the time-dependence of the paracetamol effect in the intact tissue is shown in Fig. 5 and is based on mean integral values of the ^{1}H MAS NMR spectral data of all animals as a function

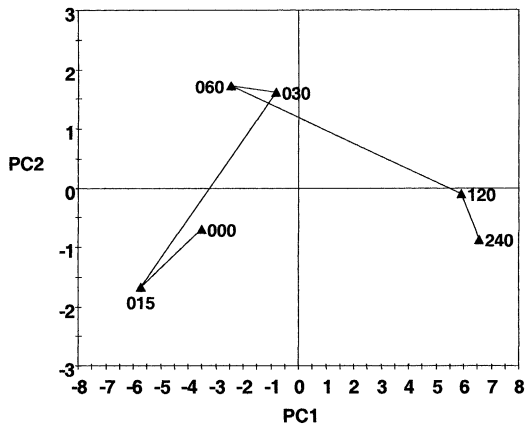

Fig. 5. Principal components trajectory plot based on ^{1}H MAS NMR spectroscopy of intact liver tissue showing the time dependence of paracetamol effects at a dose of 500 mg/kg. Key: 000-control animals; 015, 030, 060, 120, 240-animals at sampling time points of 15, 30, 60, 120, and 240 min, respectively.

of the time of euthanasia after administration. It can be seen that the profile at 15 min after dosing is closest to the control animal profile and this metabolic trajectory moves away to very similar positions at 30 and 60 min and then again to a further position where the 120 and 240 min profiles are again similar. There is no return to the control profile at the end of the experiment.

The lipid extract NMR spectra showed metabolite changes in a similar dose- and time-dependent manner as the NMR spectra of intact tissues, with significant enhancement in triglyceride levels at the mid and high doses but a large decrease in phospholipids. Assignment of the ^{1}H NMR peaks in the lipid extracts was facilitated by the measurement of a ^{1}H–^{31}P HMQC-TOCSY NMR spectrum and this is shown in Fig. 6. Detailed analysis of the ^{1}H NMR spectra of the lipid extracts also allowed assignment of a variety of different fatty acyl moieties in triglycerides and phospholipids [9]. The NMR spectra of the aqueous extracts of liver tissue from the treated animals revealed a significant decrease in the glucose peaks and the *N*-acetyl resonances of glycoproteins and an increase in the phospholipid breakdown products choline, phosphorylcholine, and glycerophosphorylcholine. There was also a marked increase in the lactate, alanine, isoleucine, leucine, lysine, tyrosine, histidine, and valine resonances.

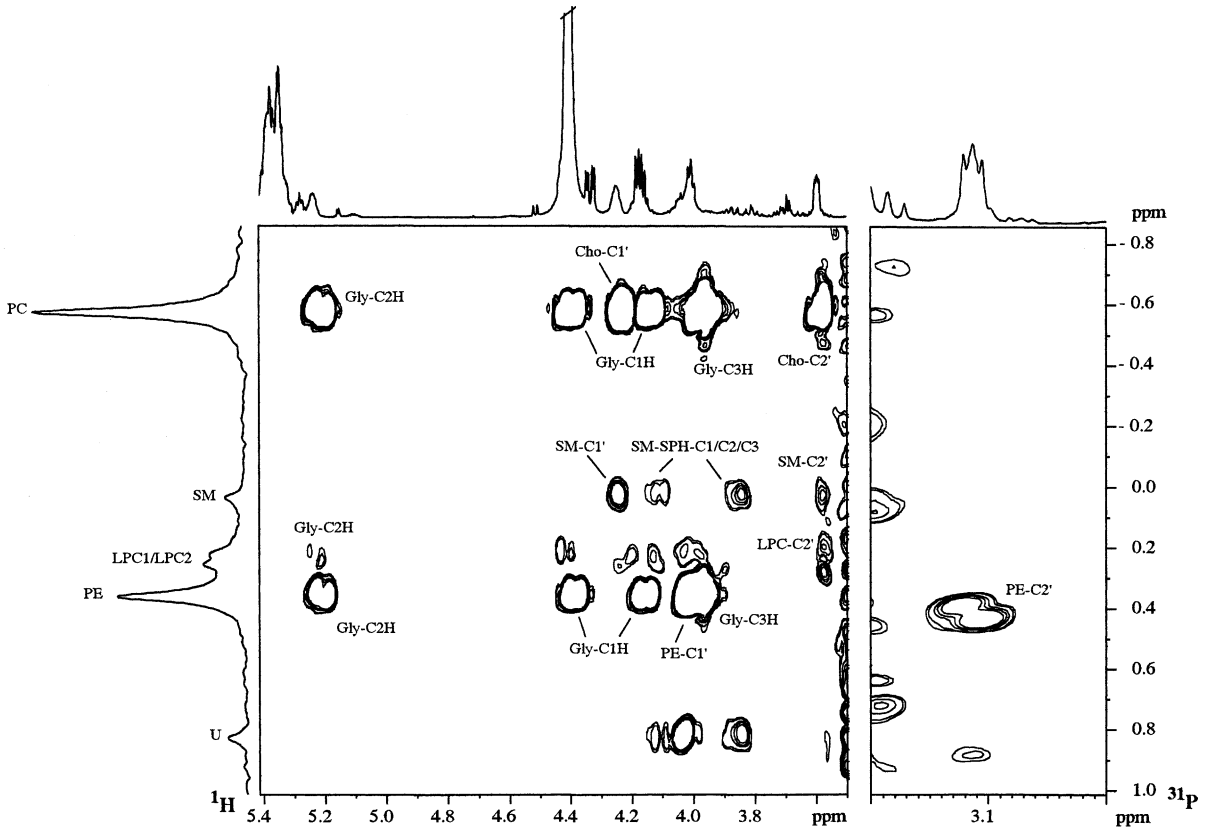

Fig. 6. Two-dimensional inverse-detected ^{1}H–^{31}P HMQC TOCSY NMR spectrum of control lipid-soluble liver tissue extract. Key: PC, phosphatidylcholine; PE, phosphatidylethanolamine; SM, sphingomyelin; LPC1, 1-acyl-lysophosphatidylcholine; LPC2, 2-acyl-lysophosphatidylcholine; U, unidentified metabolite tentatively assigned as phosphatidylinositol. Experimental parameters: 64 transients for 256 increments collected into 1 K data points with a spectral width of 6009 Hz in F2 (^{1}H) and 2429.7 Hz in F1 (^{31}P); relaxation delay, 2 s; acquisition time, 0.85 s; spin-lock, 100 ms, GARP decoupling; the data were zero-filled by a factor of 2 and a sine-bell squared apodization was applied in both dimensions; the correlations were based on $J(^{31}\mathrm{P}-^{1}\mathrm{H}) = 7$ Hz.

The ^{1}H NMR spectra of plasma showed that at the high-dose level, the concentrations of lactate, acetate, sugars, and lipids were elevated at all time points from 15 to 240 min. Pyruvate was initially decreased at 15 and 30 min, then elevated at 60, 120, and 240 min. The resonances associated with 3-D-hydroxybutyrate were also increased at the high dose levels at all time points in agreement with the 2.5 and 2.6-fold increase reported earlier in the β-hydroxybutyrate dehydrogenase protein precursor after the high dose at 30 and 60 min [20].

4. Discussion

It has previously been shown that one of the main events of paracetamol toxicity in isolated hepatocytes is an overall energy failure [25,26]. This has been further supported by a recent study using genomics and proteomics in vivo [20]. Moreover, it has been recently reported that non-toxic doses of paracetamol in fed rats, also decreased fatty acid synthesis pathways and cholesterol metabolism [27]. Now, the metabonomic analysis, which showed elevated lipid concentrations in liver tissue, tissue extracts, and plasma samples, also suggests that a shift in energy metabolism has occurred as a consequence of paracetamol hepatotoxicity. A decrease in the amounts of hepatic glucose and glycogen was observed in liver tissue, suggesting that the rate of glycogenolysis and glycolysis had increased as a consequence of lipid metabolism failure in high-dose, late time point animals. An increase in alanine and lactate concentrations in the aqueous tissue extract spectra and also an increase in lactate and pyruvate in plasma was observed. This offers further supporting evidence for the hypothesis that the cells switched to glycolysis to compensate for the loss of ATP coming from fatty acid β-oxidation. A previous study with paracetamol demonstrated severe mitochondrial changes leading to generation of megamitochondria [20] that are supposedly ATP-depleted and non-functional [28].

It is possible to focus in on certain gene expression changes and to link them to specific metabolic effects. Thus, insulin-like growth factor binding protein-1 (IGFBP-1) is structurally and functionally related to insulin and modulates actions of IGFs. IGFBP-1 has been shown to be regulated by a number of endogenous factors and insulin seems to be the main and most potent down-regulator of IGFBP-1 expression [29]. IGBP-1 has also been involved in glucose metabolism inhibition in liver [29]. Up-regulation of IGFBP-1 from 120 min onwards at the mid and high dose could indicate an attempt to increase glycogen synthesis by stabilizing IGFs on IGF-receptors, or an attempt to limit hepatic glycolysis in order to favor lipid catabolism. This would only increase the inability of hepatocytes to draw in any energy sources and precipitate more profound liver toxicity. Transgenic mice over-expressing IGFBP-1 demonstrated inhibition of IGFs metabolic effects and a high level of blood glucose [30], which was the case for high paracetamol-dosed animals here. Thus, despite the obvious alteration of glucose metabolism by paracetamol overdose and the fundamental role in glucose metabolism played by IGFBP-1, it is hard to discriminate between cause and consequence and the exact role of IGFBP-1 increase in paracetamol hepatotoxicity.

The gene coding for uteroglobin, a protein that binds phosphatidylcholine and phosphatidylinositol and which is a potent inhibitor of phospholipase-A2, was up-regulated at all time points in the mid and high dose animals (Table 2). However, from the metabonomic analysis, phospholipid levels decreased and glycerophosphorylcholine and choline levels increased indicating an overall increase in phospholipase activity. This can be explained, given the up-regulation of the gene at the late time points after the metabolic changes are seen to occur, as a compensatory mechanism whereby the liver tries to prevent further loss of phospholipids by an increase in the phospholipase inhibiting protein.

Down-regulation of lipoprotein lipase mRNA correlated with the observed increase of triglycerides in liver at all doses by NMR spectroscopy, as the primary function of this lipase is the hydrolysis of triglycerides and VLDL [31]. VLDL protein receptor mRNA was decreased most likely to counterbalance triglyceride accumulation in liver, as this receptor promotes VLDL import in cells [32]. Although mRNA of this receptor has not been detected in human liver [33], the stringency used here to call a gene present allowed the assessment of its presence in mouse liver. It has previously been shown that Apolipoprotein A4 was up-regulated at 4 h post-injection with 500 mg/kg paracetamol [34]. This enzyme has a critical role in

activation of lipoprotein lipase [33]. Thus, triglyceride accumulation in liver as shown by metabonomics was in full agreement with the decrease of lipoprotein lipase mRNA as shown through genomics, as well as compensatory mechanisms by VLDL receptor mRNA decrease and Apolipoprotein A4 protein increase as shown by proteomics [34]. In a previous study [20], it has been shown using proteomics on a mitochondrial liver fraction, that paracetamol impairs lipid metabolism by down-regulating several key enzymes involved in fatty acid β-oxidation. It was hypothesized that this would create a lack of acetyl-CoA, which could impair the Krebs cycle. This hypothesis is confirmed in the present metabonomic study by the accumulation of acetate and lactate in the blood and aqueous tissue extracts. Furthermore, the time- and dose-dependent increase of 3-D-hydroxybutyrate in blood matched the time- and dose-dependent increase of the β-hydroxybutyrate dehydrogenase observed previously [20]. Independently, it has been reported that a non-toxic dose of paracetamol in rat, disrupts fatty acid energy metabolism in liver [27]. This is further evidence that paracetamol impacts on mitochondrial function. Toxic doses of APAP would further enhance this disruption, leaving no chance of recovery to damaged hepatocytes.

This study has applied new technologies to investigate the toxicity of an old drug paracetamol, but one that still causes widespread morbidity in the human population due to abuse. Whilst the chemically-mediated initial response has not been investigated at the time points chosen for sampling, both genomics and metabonomics yield information on the cellular energy decreases which are a down-stream consequence of the initial biochemical mechanism. The various techniques yielded results which were similar in time of effect. Thus, the transcriptome and proteome were affected at the earliest time point of 15 min at the mid and high doses, and histology with electron microscopy [20] was able to detect obvious mitochondrial changes as early as 15 min post-dose. Metabonomic changes were also seen at the 60 min time point for the mid and high dose groups. In summary, metabonomics has demonstrated profound changes in glucose/glycogen and lipid metabolism that confirm the genomic and proteomic data suggesting that the consequence of paracetamol toxicity in the mouse involves a global failure in energy metabolism.

References

[1] J.K. Nicholson, J. Connelly, J.C. Lindon, E. Holmes, Nat. Rev. Drug Disc. 1 (2002) 153–161.
[2] J.K. Nicholson, J.C. Lindon, E. Holmes, Xenobiotica 29 (1999) 1181–1189.
[3] J.C. Lindon, J.K. Nicholson, E. Holmes, J.R. Everett, Concepts Magn. Reson. 12 (2000) 89–320.
[4] J.C. Lindon, J.K. Nicholson, E. Holmes, H. Antti, M.E. Bollard, H. Keun, O. Beckonert, T.M. Ebbels, M.D. Reily, D. Robertson, G.J. Stevens, P. Luke, A.P. Breau, G.H. Cantor, R.H. Bible, U. Niederhauser, H. Senn, G. Schlotterbeck, U.G. Sidelmann, S.M. Laursen, A. Tymiak, B.D. Car, L. Lehman-McKeeman, J.M. Colet, C. Thomas, Toxicol. Appl. Pharmacol. 187 (2003) 137–146.
[5] D.G. Robertson, M.D. Reily, R.E. Sigler, D.F. Wells, D.A. Paterson, T.K. Braden, Toxicol. Sci. 57 (2001) 326–337.
[6] A. Tomlins, P.J.D. Foxall, J.C. Lindon, M.J. Lynch, M. Spraul, J.R. Everett, J.K. Nicholson, Anal. Commun. 35 (1998) 113–115.
[7] N.J. Waters, E. Holmes, A. Williams, C. Waterfield, R.D. Farrant, J.K. Nicholson, Chem. Res. Toxicol. 14 (2001) 1401–1412.
[8] M.E. Bollard, S. Garrod, E. Holmes, J.C. Lindon, E. Humpfer, M. Spraul, J.K. Nicholson, Magn. Reson. Med. 44 (2000) 201–207.
[9] M. Coen, E.M. Lenz, J.K. Nicholson, I.D. Wilson, F. Pognan, J.C. Lindon, Chem. Res. Toxicol. 16 (2003) 295–303.
[10] E.M. Boyd, G.M. Bereczky, Br. J. Pharmacol. 26 (1966) 606–614.
[11] D.G. Davidson, W.N. Eastham, Br. Med. J. 5512 (1966) 497–499.
[12] D.J. Jollow, S.S. Thorgeirsson, W.Z. Potter, M. Hashimoto, J.R. Mitchell, Pharmacology 12 (1974) 251–271.
[13] J.G. Kleinma, R.V. Breitenfield, D.A. Roth, Clin. Nephrol. 14 (1980) 201–205.
[14] D.C. Dahlin, G.T. Miwa, A. Lu, S.D. Nelson, Proc. Natl. Acad. Sci. U.S.A. 81 (1984) 1327–1331.
[15] J.O. Miners, R. Drew, D.J. Birkett, Biochem. Pharmacol. 33 (1984) 2995–3000.
[16] J.R. Bales, J.D. Bell, J.K. Nicholson, P.J. Sadler, J.A. Timbrell, R.D. Hughes, P.N. Bennett, R. Williams, Magn. Reson. Med. 6 (1988) 300–306.
[17] P. Chomczynski, K. Mackey, Biotechniques 19 (1995) 942–945.
[18] R.J. Lipshutz, S.P. Fodor, T.R. Gingeras, D.J. Lockhart, Nat. Genet. 21 (1999) 20–24.
[19] D.J. Lockhart, H. Dong, M.C. Byrne, M.T. Follettie, M.V. Gallo, M.S. Chee, M. Mittmann, C. Wang, M. Kobayashi, H. Horton, E.L. Brown, Nat. Biotechnol. 14 (1996) 1675–1680.
[20] S.U. Ruepp, R.P. Tonge, J. Shaw, N. Wallis, F. Pognan, Toxicol. Sci. 65 (2002) 135–150.
[21] T.P. Reilly, M. Bourdi, J.N. Brady, C.A. Pise-Masison, M.F. Radonovich, J.W. George, L.R. Pohl, Biochem. Biophys. Res. Commun. 282 (2001) 321–328.
[22] K.P.R. Gartland, C.R. Beddell, J.C. Lindon, J.K. Nicholson, Mol. Pharmacol. 39 (1991) 629–642.

[23] E. Holmes, F.W. Bonner, B.C. Sweatman, J.C. Lindon, C.R. Beddell, E. Rahr, J.K. Nicholson, Mol. Pharmacol. 42 (1992) 922–930.
[24] J.C. Lindon, E. Holmes, J.K. Nicholson, Prog. Nucl. Magn. Reson. Spectrosc. 39 (2001) 1–40.
[25] B.S. Andersson, M. Rundgren, S.D. Nelson, S. Harder, Chem. Biol. Interact. 75 (1990) 201–211.
[26] P.C. Burcham, A.W. Harman, J. Biol. Chem. 266 (1991) 5049–5054.
[27] R. Irwin, G.A. Boorman, R. Paules, A. Heinloth, R.W. Tennant, M.L. Snell, M.L. Cunningham, Tox. Sci. 72 (S-1) (2003) 340.
[28] M. Karbowski, C. Kurono, M. Wozniak, M. Ostrowski, M. Teranishi, Y. Nishizawa, J. Usukara, T. Soji, T. Wakabayashi, Free Radical Biol. Med. 26 (1999) 396–409.
[29] P.D.K. Lee, L.C. Giudice, C.A. Conover, D.R. Powell, Proc. Soc. Exp. Biol. Med. 216 (1997) 319–357.
[30] L.J. Murphy, Pediatr. Nephrol. 14 (2000) 567–571.
[31] A. Niemeier, M. Gafvels, J. Heeren, N. Meyer, B. Angelin, U. Beisiegel, J. Lipid Res. 37 (1996) 1733–1742.
[32] J.C. Webb, D.D. Patel, M.D. Jones, B.L. Knight, A.K. Soutar, Hum. Mol. Genet. 3 (1994) 531–537.
[33] I.J. Goldberg, C.A. Scheraldi, L.K. Yacoub, U. Saxena, C.L. Bisgaier, J. Biol. Chem. 265 (1990) 4266–4272.
[34] R. Tonge, J. Shaw, B. Middleton, R. Rowlinson, S. Rayner, J. Young, F. Pognan, E. Hawkins, I. Currie, M. Davison, Proteomics 1 (2001) 377–396.